Algerian Journal of Engineering and Technology 01 (2019) 019–024

Algerian Journal of Engineering and Technology

Journal homepage: https://jetjournal.org/index.php/ajet

Original Article

Broken rotor bars fault detection in induction motors using FFT: simulation and experimentally study

Ridha Kechida[a,*], Arezki Menacer[b], Hakima Cherif[a]

[a]Faculty of Technology, University of El-oued, PO Box 789 El-oued 39000, Algeria
[b]LGEB Laboratory Department of Electrical Engineering, University of Biskra, Algeria

ARTICLE INFO

Article history:
Received 11 September 2019
Revised 12 October 2019
Accepted 14 October 2019

Keywords:
Induction Motors;
Broken Rotor Bars;
FFT;
Fault Diagnosis.

ABSTRACT

This paper presents the fault detection of broken rotor bars based on the analysis technique, such as the fast Fourier transform (FFT), which utilize the steady-state spectral components of the stator quantities is considered. This technique has been given expected results, the accuracy of this technique depends on the loading conditions and constant speed of the motor. This method shows good theoretical and experimental results

1. Introduction

The induction motors often operate in hostile environments such as corrosive and dusty places. They are also exposed to a variety of undesirable conditions. These unwanted conditions can cause the induction motor to go into a premature failure period, which may result in an unserviceable condition of the motor, if not detected in its early stages of the failure period [1]. The failure of induction motors can result in a total loss of the machine itself. Thus, health monitoring techniques to prevent induction motor failures are of great concern in the industry and are gaining increasing attention [1, 2]. Rotor failures are among these failures. Several monitoring techniques have been developed, most of which are based on motor current signature analysis (MCSA) [3-5].

MCSA (Motor Current Signature Analysis) is one of the most widely used techniques in the fault detection analysis of induction machines [6]. MCSA focuses its efforts in the spectral analysis of the stator current and has been successfully used in the detection of broken rotor bars, and dynamic eccentricity [7–13]. The procedure consists of evaluating the relative amplitude of current harmonics that appear due to this defect [14]. The advantage of this technique is that it is well recognized nowadays as a standard due to its simplicity: It needs only one current sensor per machine and is based on straightforward signal-processing techniques such as fast Fourier transforms (FFT). However, it has mainly been designed for fixed frequency supply, such as for machines connected to the electrical grid [6].

* Corresponding author.
E-mail address: ridha-kechida@univ-eloued.dz
Peer review under responsibility of University of Echahid Hamma Lakhdar.
https://doi.org/10.5281/zenodo.3595143

In this paper, a method based on the current and a speed signature analysis of broken rotor bars is used. The approach is also compared with the well-known Fourier method for the analysis of the stator current in steady state operation. Several experiments are developed for different fault cases such as healthy rotor and two broken rotor bars.

2. Motor Current Signature Analysis

2.1. 2.1. *Broken Rotor Bar fault*

Rotor failures account for 5–10% of induction motor problems [15-16]. A broken rotor bar fault has distinctive characteristic frequencies which can be calculated as:

$$f_{defect} = \left(1 \pm 2\mathrm{ns}\right) f, \quad \mathrm{k} = 1, 2, ... \quad (1)$$

Where *f*: is the driving frequency and *s*: is the fractional slip of the motor.

Once there is a broken rotor bar fault, sidebands around the driving frequency can be expected in the power spectrum. In particular, the first-order sidebands (e.g. n=1) are of particular interest in the detection of broken rotor bar fault. The left sideband (1-2ns)*f* is due to electrical or magnetic rotor asymmetry caused by broken rotor bars while the right sideband (1+2ns)*f* is due to the speed ripple or variation. The amplitudes and presence of the sidebands depend on the physical position of the broken rotor bars, speed, and load. The locations of the sidebands will shift outwards as the speed and load are increased. It is acknowledged that the sidebands may also be observed when the motor has no broken rotor bar fault as rotor ellipticity and shaft misalignment could both induce rotor asymmetry to a certain extent [17].

3. Model of Induction Motor With fault: Broken Rotor Bars

The model of a three-phase induction motor in the reference frame (d-q) related to the rotor is [2]:

$$\begin{cases} \dot{x}(t) = A(\omega).\, x(t) + B.u(t) \\ y(t) = C.x(t) \end{cases} \quad (2)$$

with: $x = \begin{bmatrix} i_{ds} & i_{qs} & \phi_{dr} & \phi_{qr} \end{bmatrix}^{\mathrm{T}}$, $u = \begin{bmatrix} U_{ds} & U_{qs} \end{bmatrix}^{\mathrm{T}}$, $y = \begin{bmatrix} i_{ds} & i_{qs} \end{bmatrix}^{\mathrm{T}}$

$$A(x) = \begin{bmatrix} -(R_s + R_{eq})L_f^{-1} & \omega_r & R_{eq}L_m^{-1}L_f^{-1} & \omega_r L_f^{-1} \\ -\omega_r & -(R_s + R_{eq})L_f^{-1} & \omega_r L_f^{-1} & R_{eq}L_m^{-1}L_f^{-1} \\ R_{eq} & 0 & R_{eq}L_m^{-1} & 0 \\ 0 & R_{eq} & 0 & -R_{eq}L_m^{-1} \end{bmatrix} \quad B = \begin{bmatrix} L_f^{-1} & 0 \\ 0 & L_f^{-1} \\ 0 & 0 \\ 0 & 0 \end{bmatrix},$$

and:

$$R_{eq} = R_r - \frac{\alpha}{1+\alpha} Q(\theta_0) R_r \,, \quad \alpha = \frac{2}{3}\eta_0 \,, \eta_0 = \frac{3n_{bc}}{n_b} \,, \quad Q(\theta_0) = \begin{bmatrix} cos(\theta_0)^2 & cos(\theta_0)sin(\theta_0) \\ cos(\theta_0)sin(\theta_0) & sin(\theta_0)^2 \end{bmatrix}$$

With:

n_{bc} and n_b represent the number of broken bars and the total number of bars in the rotor.

θ_0: an absolute localization of the faulty winding according to the first rotor phase.

The expression of the torque is given:

$$T_e = p(i_{qs}\, \phi_{dr} - i_{ds}\, \phi_{qr}) \quad (3)$$

4. Simulation And Experimental Results

The motor under experimental test is 1.1 kW, 220/380V, 50 Hz, 4 pole, Squirrel-cage induction motor with 28 rotor bars, a DC generator acts as a load. Two types of signals are collected in the experiments: stator current and stator voltage. The signals were interfaced to a PC by A Data acquisition board.

Fig. 1. Experimental test bench

4.1. Fast Fourier Transform (FFT) Analysis

Figure 2 shows the stator current and speed at steady state for loading machine of simulation analysis and experimental results. We can notice a good agreement between the results. The oscillations shown by the curves of the stator current and speed, justify the presence of a break rotor bar defect in the machine.

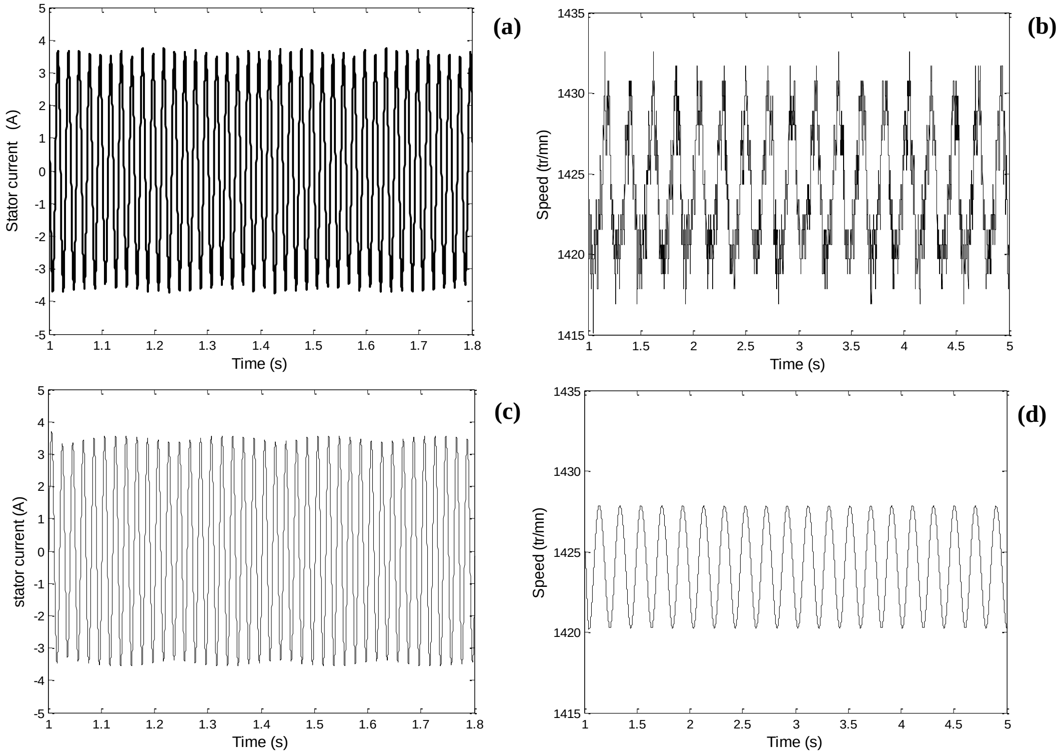

Fig. 2 Stator current and speed for faulty induction motor with two broken rotor bars:

(a, b) experimental result, (c, d) simulation results

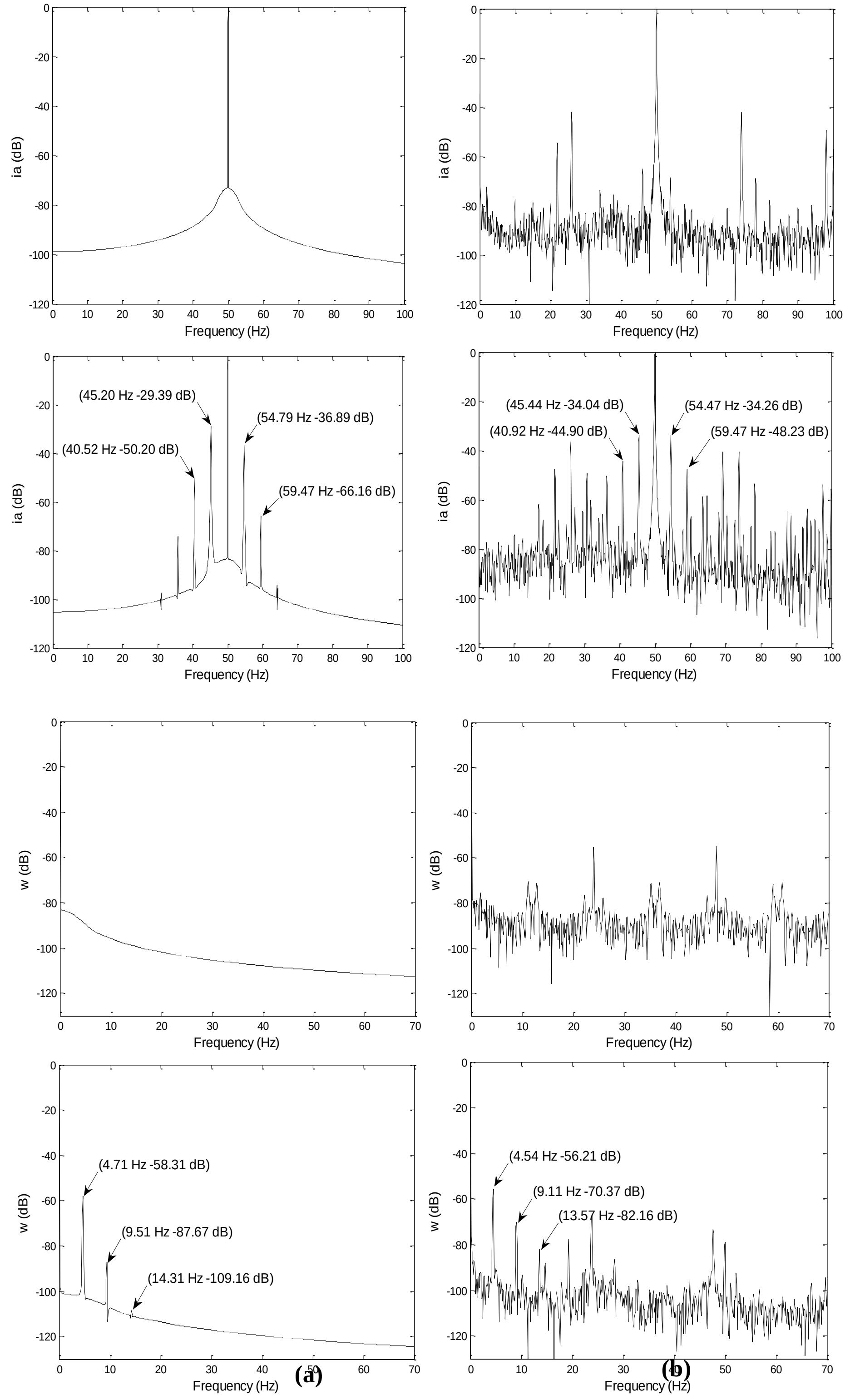

Fig.3. The stator current and speed spectrum for healthy and two broken bars motor (s=4.3%): (a) simulation and (b) experimental results.

Figure 3 shows the comparison of frequency spectrums resulted from the computer simulation and experimental measurements of induction motor under the conditions of two broken bars and healthy motor. It is obvious that, the magnitude of the components $(1\pm2s)f$ and $2sf$ are increased by increments of nonsymmetrical condition in rotor from the healthy state to the state of two broken bars (experimental results). The result of rotor broken bars, see an increase in the magnitude of the harmonics amplitude of the stator current and speed spectrum.

Table 1 Frequencies and magnitudes of the stator current spectrum

Machine 1.1 Kw		(1-4s)f	(1-2s)f	(1+2s)f	(1+4s)f
Simulation s≈4.3%	f (Hz)	40.52	45.20	54.79	59.47
	Mag (dB)	-50.20	-29.39	-36.89	-66.16
Experimental s≈4.4%	f (Hz)	40.92	45.44	54.47	59.57
	Mag(dB)	-44.90	-34.04	-34.26	-48.23

5. Conclusion

The spectrum analysis methods are among the motor current signature analysis (MCSA) techniques used for broken rotor bar fault detection and diagnosis in induction motors. The work presented in this paper deals with the application of the spectral analysis of stator current and speed of an induction motor. The stator current spectrum analysis shows the presence of a defect due to the broken of bars resulted in appearance of different harmonics on both sides of the fundamental. The experimental and simulated results show that rotor cage faults can be effectively detected by this technique. Also the experiments have clearly demonstrated the effectiveness of speed spectrum in cage rotor fault detection whose relies on the behaviour of the spectral component at frequency of $2sf$.

Appendix

For the simulated induction motor

P output power	1.1 kW
Vs stator voltage	220/380 V
Is nominal current	2.6/4.3 A
nn nominal speed	1425 rpm
Rs stator resistance	9.81 Ω
Rr rotor resistance	3.83 Ω
Lm mutual inductance	436 mH
Lf leakage inductance of stator	76.2 mH
p number of pole pairs	2
n number of stator slots	48
nb number of rotor bars	28
ns number of turns per stator phase	464

References

1. Ayhan, B. Trussell, H.J. Chow, Mo-Yuen. Song, Myung-Hyun (2008). On the use of a lower sampling rate for broke rotor bar detection with DTFT and AR-based spectrum methods. *IEEE Trans. Industrial Electronics*, 55(3), 1421-1434.
2. Bachir, S. Tnani, S Trigeassou. J-C. and Champenois, G. (2006). Diagnosis by parameter estimation of stator and rotor faults occurring in induction machines. *IEEE Transitions Industrial Electronics*, 53(3), 963–973.
3. Bellini, A. Filippetti, F. Tassoni, C. and Capolino. G.A. (2008). Advances in diagnostic techniques for induction machines. *IEEE Transactions on Industrial Electronics*, 55(12), 4109-4125.
4. Silva, A.M.D. Povinelli, R. J. and Demerdash, N. A. O. (2008). Induction machine broken bar and stator short-circuit fault diagnostics based on three-phase stator current envelopes. *IEEE Transactions on Industrial Electronics*, 55(3), 1310–1318.

5. Bossio, G. R. De Angelo, C. Bossio, H. J. M. Pezzani, C. M. and García, G.O.(2009). Separating broken rotor bars and load oscillations on im fault diagnosis through the instantaneous active and reactive currents. *IEEE Transactions on Industrial Electronics,* 56(11), 4571–4580.
6. Bouzida, A. Touhami, O. Ibtiouen, R. Belouchrani, A. Fadel, M. and Rezzoug, A. (2011). Fault Diagnosis in industrial induction Machines through Discrete Wavelet Transform. *IEEE Transactions Industrial Electronics,* 58(9), 4385–4395.
7. Sadeghian, A. Ye, Z. and Wu, B. (2009). Online detection of broken rotor bars in induction motors by wavelet packet decomposition and artificial neural networks. *IEEE Transactions Instrumentation and Measurement,* 58(7), 2253-2263.
8. Cusidó, J. Romeral, L. Ortega, J. A. Rosero, J. A. Garcia Espinosa, A. (2008). Fault detection in induction machines using power spectral density in wavelet decomposition. *IEEE Trans. Industrial Electronics,* 55(3), 633-643.
9. Zhou, W. Habetler, T. G. and Harley, R.G. (2007). Stator current based bearing fault detection techniques: A general review, *IEEE international Symposium on Diagnostics for Electric Machines, Power Electronics and Drives*, pp. 7-10.
10. Blodt, M. Granjon, P. Raison, B. Rostaing, G. (2008). Models for bearing damage detection in induction motors using stator current monitoring. *IEEE Transactions on Industrial Electronics,* 55(4), 1813-1822.
11. Douglas, H. Pillay, P and Ziarani, A. K. (2005). Broken rotor bar detection in induction machines with transient operating speeds. *IEEE Transactions on Energy Conversion,* 20(1), 135-141.
12. Antonio-Daviu, J.A. Riera-Guasp, M. Floch, J. R. Palomares, M.P.M. (2006). Validation of a new method for the diagnosis of rotor bar failures via wavelet transform in industrial induction machines. *IEEE Transactions on Industry Applications*, 42(4), 990–996.
13. Ordaz-Moreno, A. Romero-Troncoso, R.J. Vite-Frias, J.A. Rivera-Gillen, J.R. Garcia-Perez, A. (2008). Automatic online diagnosis algorithm for broken-bar detection on induction motors based on discrete wavelet transform for FPGA implementation. *IEEE Transactions on Industrial Electronics,* 55(5), 2193-2202.
14. Cusido, J. Rosero, J. Aldabas, E. Ortega, L. Romeral, J.A. (2006). New fault detection techniques for induction motors. *Electrical Power Utilization Quality and, Magazine,* 11(1), 39-45.
15. Caruso, G. Iannuzzi, D. Maceri, F. Pagano, E. Piegari, L. (2008). Torsional eigenfrequency identification of squirrel cage rotors of induction motors. *International Symposium on Power Electronics, Electrical Drives, Automation and Motion*, 1271–1275.
16. Benbouzid, M.E.H. (2000). A review of induction motors signature analysis as a medium for faults detection. *IEEE Trans Indus Elect,* 47(5), 984–993.
17. Li, W. (2006). Detection of induction motor faults: A comparison of stator current, vibration and acoustic methods. *Journal of Vibration and Control*. 12(2). 165.

Recommended Citation

Kechida, R., Menacer, A., Cherif, H. (2019). Broken Rotor Bars Fault Detection in Induction Motors using FFT: Simulation and Experimentally Study. *Algerian Journal of Engineering and Technology*, 1(1), 019-024. https://doi.org/10.5281/zenodo.3595143